

CEBAF Program Advisory Committee Six (PAC6) Proposal Cover Sheet

This proposal must be received by close of business on April 5, 1993 at:

CEBAF
User Liaison Office
12000 Jefferson Avenue
Newport News, VA 23606

Proposal Title

SEARCH FOR COLOR COHERENT EFFECTS
VIA THE OBSERVATION OF
DOUBLE SCATTERING EVENTS IN CLAS

Contact Person

Name: Kim Sh. Egiyan
Institution: Yerevan Physics Institute
Address: Alikhanian Brothers St. 2
Address:
City, State ZIP/Country: Yerevan, Armenia 375036
Phone: (804)249-7100 **FAX:** (804) 249-5800
E-Mail → BITnet: Egiyan@CEBAF.gov **Internet:**

If this proposal is based on a previously submitted proposal or letter-of-intent, give the number, title and date:

CEBAF Use Only

Receipt Date: 2/4/93 Log Number Assigned: PR 93-001

By: P

Search for Color Coherent Effects via the Observation of Double Scattering Events in CLAS

List of Participants

W.K. Brooks, V.D. Burkert, B.A. Mecking, M.D. Mestayer
B. Niczyporuk, E.S. Smith, and A. Yegneswaran
CEBAF, Newport News, Virginia

M.I. Strikman
Pennsylvania State University, Philadelphia

L.L. Frankfurt, W.R. Greenberg, G.A. Miller
University of Washington, Seattle

M.J. Amaryan, R.A. Demirchyan, K.Sh. Egiyan (spokesman)
M.M. Sargsyan, Yu.G. Sharabyan, S. Stepanyan
Yerevan Physics Institute, Armenia

Search for Color Coherent Effects via the Observation of Double Scattering Events in CLAS

Summary

We propose to investigate Color Coherent effects at intermediate values of Q^2 (\sim few $(GeV/c)^2$) using a new method of measurement. The idea is to measure the Q^2 dependence of the final state interactions of recoiling protons in quasi-elastic electron scattering from light nuclei. This method is complementary to the usual measurement of the event rate without final state interactions. Calculations show that significant color transparency effects could occur for this rescattering phenomenon at energies initially available at CEBAF. The price to pay is the effort needed to detect more than one hadron in the final state. Such processes have small cross sections, so the use of large acceptance (4π) detectors like CLAS is necessary.

Introduction

One of interesting directions to investigate QCD is to study the interface between perturbative (short distance) and non-perturbative (large distance) QCD instead of the study of the reasonably well understood purely perturbative regime. The most popular reaction, where the relative role of perturbative and non-perturbative contributions has been actively discussed for a long time, is elastic electron-nucleon scattering. Both the proponents and opponents of the idea that perturbative QCD effects are dominant have presented interesting arguments. Another approach to understand this region is to examine models of the nucleon to determine those that allow a small size configuration or a point-like configuration (PLC) to develop at not too large Q^2 . (The PLC is a precursor of the dominance of pQCD.) The result is that realistic quark models of a nucleon which contain a Coulomb type interaction at small interquark distances and Skyrmin models both allow a PLC to form at a momentum transfer as small as 1-2 $(GeV/c)^2$ (see analysis made in [1,2]). The opposite behavior is expected in mean-field quark-models of the nucleon, and in chiral Lagrangian models where a nucleon is considered as a structureless particle surrounded by a meson cloud.

Thus, the pressing problem now is to find experimental evidence that helps to distinguish between these two classes of models. The ideas of pQCD lead to the suggestion [3,4] that the A-dependence of quasi-exclusive processes

$$l(h) + A \rightarrow l(h) + p + (A - 1) \quad (1)$$

could be used to determine the configurations that dominate in hard two-body reactions. The notion was to explore the color screening phenomenon in QCD - the decrease of

the interaction with a decrease of the transverse area, S , occupied by the color charge: $\sigma \sim S$ for $S < \pi r_t^2$. For the interaction of a small-sized object, the color screening effect would allow its escape from the nucleus without further interactions. Hence, the cross section of reaction (1) would be proportional to A . This is the Color Transparency (CT) phenomenon. The prediction of a spectacular change of A -dependence of the cross section of reaction (1) has led to a number of further theoretical analyses [5-9] and to first attempts to observe the phenomenon using the BNL proton beam [10] and several ongoing experimental investigations at SLAC [11] and BNL [12].

The practical problem which emerges in looking for this phenomenon is that the PLC expand rapidly (even if they are selected at the interaction point) to the size of a normal hadron while propagating through the nucleus. This is because the PLCs are not eigenstates of the QCD Hamiltonian. This expansion (quantum diffusion) of the wave packet dominates up to rather large Q^2 because of the relatively small Lorentz factor of the struck nucleon [5]. The expansion length L can be estimated as follows [5]:

$$L(fm) \sim \frac{2p_N}{\delta m^2} \quad (2)$$

where δm^2 characterizes the differences of mass squared that appear in the nucleon excitation spectrum. The realistic range of δm^2 is between m_ρ^2 and $\frac{1}{\alpha'}$ ($\alpha'=0.9 \text{ GeV}^{-2}$ is the slope of the nucleon Regge trajectory). Thus Eq. (2) can be rewritten as

$$L(fm) \sim l_0(fm) \cdot (p_N(GeV/c)), \quad l_0 = 0.35 \div 0.55 fm \quad (2')$$

In the following estimates, we will adopt the more optimistic value of $l_0 = 0.5 fm$. Choosing l_0 in the lower end of the range would correspond to rescaling Q^2 by approximately a factor of 1.5, say $Q^2 = 4(GeV/c)^2$ to $Q^2 = 6(GeV/c)^2$. Since in reaction (1) $p_N = \sqrt{Q^2 + (Q^2/2m)^2}$ the change of A_{eff}/A in this process is expected to be rather small up to $Q^2 \sim 10(GeV/c)^2$. Therefore, to establish CT in reactions like $A(e, e'p)$, very large values of Q^2 are necessary. This expectation is consistent with the recent data from the SLAC experiment NE18 [11] which do not observe a change of A_{eff}/A at their current level of accuracy ($\sim 20\%$) up to $Q^2 \sim 7(GeV/c)^2$. There are further uncertainties in the interpretation of the $A(e, e'p)$ experiments due to the role of off-energy-shell effects in nucleon form factors.

We propose to investigate Color Coherent effects at intermediate Q^2 (\sim few $(GeV/c)^2$) using a new method of measurement. The idea is to measure the Q^2 dependence of the number of final state interaction events (instead of non-interacting events) of the outgoing protons in reaction (1). Our calculations show that, for this reaction, the (relative) Color Transparency effects are enhanced to a measurable value at $Q^2 \leq 4(GeV/c)^2$ using the lightest nuclei. Due to the small cross sections and the need for detecting more than one hadron in the final state of the reaction (1), the use of large acceptance (4π) detectors is necessary. These problems may be solved using the CLAS detector.

2. Physics Motivation

2.1. The Idea

To observe CT at intermediate values of Q^2 it is necessary to suppress the effects of wave packet expansion. This can be achieved by using the lightest nuclear targets, where distances are small. Then, color coherent effects manifest themselves as a decrease of the probability for final state interactions with increasing Q^2 . The classical method to observe this phenomenon is the measurement of the number of the non-interacting recoiling protons in reaction (1) (Fig. 1a) as a function of Q^2 .

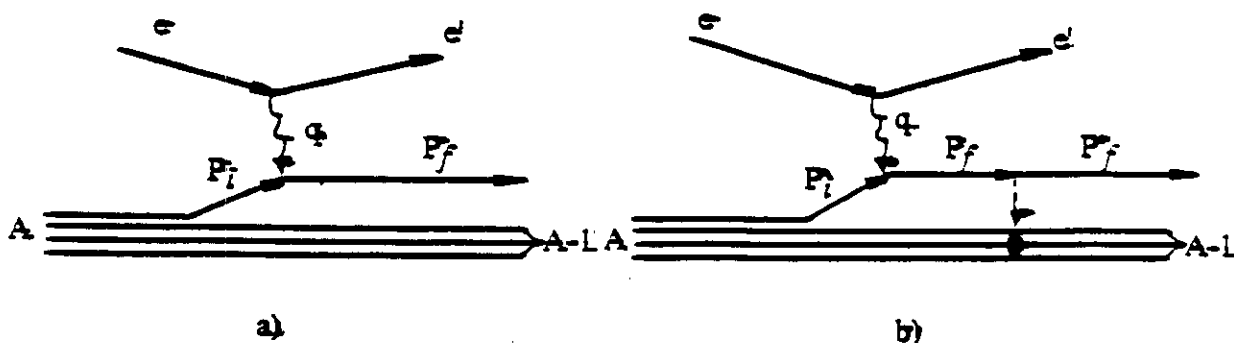


Fig. 1

Experiments of this type are technically feasible, but the effect to be measured is small, especially at $Q^2 \leq 4 - 5(\text{GeV}/c)^2$. For illustration, the Q^2 dependence of the ratio

$$R \equiv \frac{A_{eff}}{A} \quad (3)$$

for ${}^4\text{He}$ and ${}^{12}\text{C}$ is displayed in Fig. 2a and 3a. (For the ${}^{12}\text{C}$ nucleus, similar results have been obtained by others [6,8,9,13]). The solid histogram represents results without color transparency effects (Glauber approach). One can see that the effect to be measured is no larger than 10% at $Q^2 = 4(\text{GeV}/c)^2$ growing to only 30% at $10(\text{GeV}/c)^2$. Therefore, the effect will be difficult to measure at a beam energy of 4 - 6 GeV, and to distinguish the CT effect from off-shell-effects in the elementary amplitudes.

We propose a different way to detect the final state interaction in (1), suggested in [14], in which the expected effect is enhanced. Instead of looking for events where no secondary interaction has occurred (Fig. 1a), one can look for events where the struck nucleon interacts with the residual nucleus (Fig. 1b). In the first case, we seek an effect that increases asymptotically by no more than a factor ~ 1.5 , while in the second case

we may observe an effect of the cross section decreasing from some finite value to zero in asymptotia, i.e. for an effect which is changing by a large factor.

One can expect a significant effect at finite values of Q^2 if the expansion length L becomes comparable to the nuclear size. For instance, at $Q^2 = 4(\text{GeV}/c)^2$ (accessible with a 4 GeV energy beam), $L \approx 1.5$ fm (see eq. (2)), which is comparable to the radius of the ${}^4\text{He}$ nucleus (1.7 fm), while at $Q^2 = 6(\text{GeV}/c)^2$ (feasible for the 6 GeV beam energy), $L \approx 2$ fm which is close to the radius of the ${}^{12}\text{C}$ nucleus (2.2 fm). Thus, the suggested regime can be achieved using the lightest targets at $Q^2 \leq 4 \div 6(\text{GeV}/c)^2$. This is illustrated in Fig. 2b and 3b [15], where the Q^2 dependences of the quantity

$$1 - R$$

are presented, $(1-R)$ is proportional to the fraction of interactions where the struck protons scatter off the residual $(A-1)$ nucleus.

One can see that CT effects are larger for $(1-R)$ than for R (for ${}^4\text{He}$, by a factor ~ 2 at $Q^2 \approx 4(\text{GeV}/c)^2$, and by a factor ~ 1.5 at $Q^2 \geq 6(\text{GeV}/c)^2$).

A further increase of the CT effect can be achieved [15] by measuring events involving both interacting and non-interacting recoil final state protons, i.e. by the investigation of both reactions:



In (4) and (5) p_f , p'_f and p_r represents non-interacting recoil, elastically scattered and secondary protons, respectively. In this case, the ratio

$$\frac{1 - R}{R} \quad (6)$$

can be obtained. This quantity is evidently more sensitive to the Color Transparency effect. In addition, uncertainties in the off-energy-shell eN amplitudes cancel out to a large extent in this ratio. The same is true for the suppression of point-like configurations in bound nucleons which significantly changes the Q^2 -dependence of R [16]. This is illustrated in Fig. 2c and 3c. One can see that in this case, the CT effects increase, e.g. for ${}^4\text{He}$, by a factor of ~ 3 (relative to the R -dependence) at $Q^2 \approx 4(\text{GeV}/c)^2$ and by factor ~ 2 at $Q^2 \geq 6(\text{GeV}/c)^2$ (the corresponding deviations from the Glauber predictions are 40% and 65%).

Thus, Color Coherent effects increase to measurable values in the momentum transfer region around $4(\text{GeV}/c)^2$. The effect can be studied by measuring the flux of the (final state) interacting and non-interacting protons, produced in the quasi-elastic electron scattering. These measurements can be carried out even at the first stage of CEBAF beam energy (4 GeV). The price to be paid is the necessary measurement of a small total

cross section (due to the small probability of rescattering in the lightest nuclei) which also decreases with increasing Q^2 . The experimental problems can be solved using 4π -type detectors, in particular the CLAS detector at CEBAF.

2.2. Measurement Method

It is difficult to measure the total proton-nucleon cross section for all interaction channels, e.g. the excitation of the (A-1) system, the production of neutral particles, and the production of a meson and nucleon resonances. A more practical approach is to study some selected reaction channels. This does not lead to a reduction of the Color Transparency effect, since one could study Color Transparency for any of the channels.

It is reasonable to start by considering the elastic channel of recoil proton interaction with individual nucleons in the A-1 nucleus. To obtain the ratio (6) for this channel, one may relate the elastic to the total cross section for non-zero momentum transfer t in a manner consistent with the optical theorem:

$$\sigma_{el}(t, l, Q^2) = \frac{\sigma_{tot}^2(l, Q^2)}{16\pi} \cdot e^{bt} \cdot \frac{G_N^2(t \cdot \sigma_{tot}(l, Q^2)/\sigma_{tot})}{G_N^2(t)} \quad (7)$$

Here $\sigma_{el}(t, l, Q^2)$ is the cross section of elastic scattering for the PLC at momentum transfer t , at distance l from the point where the photon was absorbed, σ_{tot} is the proton-nucleon total cross section, b is the slope of the elastic NN amplitude, $G_N(t)$ is the Sachs form factor, and $G_N(t) \simeq \frac{1}{(1+t/0.71)^2}$. We fixed $\sigma_{el}(t, l, Q^2)$ using the optical theorem, and the difference between elastic scattering in PLC and in an average configuration was taken into account, based on the observation that $d\sigma^{(h+N \rightarrow h+N)}/dt \sim G_h^2(t) \cdot G_N^2(t)$ at intermediate energies (the last factor in Eq. (7)). In (7) $\sigma_{tot}(l, Q^2)$ is the effective total cross section of the interaction of the expanding PLC at the distance l from the interaction point. It can be estimated as [5]

$$\sigma_{tot}(l, Q^2) = [\sigma(Q^2) + (\sigma_{tot} - \sigma_{tot}(Q^2)) \cdot \frac{l}{L}] \theta(L - l) + \sigma_{tot} \cdot \theta(l - L) \quad (8)$$

The cross section at the interaction point, $\sigma(Q^2) \simeq \sigma_{tot} \cdot \frac{Q_0^2}{Q^2}$, where we take $Q_0^2 = 1(\text{GeV}/c)^2$. The calculated results are not sensitive to Q_0^2 for $Q^2 \gg Q_0^2$, since in this case uncertainties of the expansion parameters are dominant.

If we select the kinematics such that $|t| \ll 0.71(\text{GeV}/c)^2$, it is easy to see that for $l < L$ the cross section σ_{el} is suppressed much stronger than σ_{tot} . Therefore, the effect of CT for

$$\frac{N_{el}}{N_R}$$

should be significantly larger than for

$$\frac{N_{tot}}{N_R}$$

This is illustrated in Fig. 4 (${}^4\text{He}$) and Fig. 5 (${}^{12}\text{C}$) via the Q^2 dependence of the quantities $R_{el} = \frac{N_{el}}{N_{tot}}$ (4a,5a) and $\frac{R_{el}}{R} = \frac{N_{el}}{N_R}$ (4b,5b). Calculations were carried out for $|t| \geq 0.1(\text{GeV}/c)^2$.

Ratios of computed cross sections are displayed in Fig. 6 and 7. The cross sections obtained with CT effects are divided by those obtained from the conventional Glauber approach. In each case, the ratio drops significantly if $Q^2 \geq 2\text{GeV}^2$.

We also present results for the reaction

$$e + {}^3\text{He} \rightarrow e' + p'_f(N_f'^*) + p_r(400\text{MeV}/c) + n. \quad (10)$$

Here the kinematics are chosen such that the final fast proton or N^* is produced quasi-elastically and that the recoil proton has a momentum $p_r = 400\text{MeV}/c$. At this fairly large momentum value, the recoiling proton is almost certainly produced as a result of a final state interaction.

The conventional theoretical approach is to compute the matrix element of $T_2 G J_1$, where the photon is absorbed on nucleon 1 (with the operator J_1) leading to the nucleon propagating to the position of the second nucleon where the final state interaction takes place.

In color transparency physics, the absorption of the photon leads to the formation of a PLC which propagates to a second nucleon and interacts. The PLC is a wave packet which can, if so desired, be described as a coherent sum of baryonic states. In the present evaluation, the model of Ref. [16] has been used. The PLC are described as a coherent sum of three states: the nucleon N , a low mass baryon resonance N^* , and a "resonance" of higher mass N^{**} . The latter term is meant to provide a representation of the continuum. In this model, the final state interaction is a baryon-nucleon interaction represented by a three-by-three matrix. Thus, one can compute processes involving the quasi-elastic production of resonances (N^*, N^{**}) as well as protons.

The results are shown in Figs. 8 and 9. The difference between the figures is that two different sets of resonance masses have been used: 1.4 GeV and 1.8 GeV in Fig. 8, and 1.7 GeV and 3 GeV in Fig 9. In each case, the ratio of cross sections $\sigma_{CT}/\sigma_{\text{Glauber}}$ drops rapidly as Q^2 increases. (We denote the conventional cross section as "Glauber", but use the exact propagator (not the eikonal approximation) to describe the propagation of the PLC.)

Thus, Color Transparency phenomena can be investigated already at relatively small momentum transfer ($\leq 4 \div 6\text{GeV}^2$) in the quasi-elastic electron scattering process with light nuclei via the direct detection of the (final state) non-interacting and elastically scattered recoil protons.

Note that there are interesting problems left for future discussion. For example, other channels of the recoil proton interaction, e.g. the Δ -production channel that has a larger partial cross section than the elastic channel. Another aspect which requires further study

is the contribution of the nucleon-nucleon correlations in final state interactions [9]. We will return to these problems in the future development of this proposal.

3. Kinematics

We propose to study the reactions (4) and (5):

- in the quasi-elastic scattering region,
- in the $Q^2 = 1 \div 4(\text{GeV}/c)^2$ interval,
- at 4 GeV beam energy,
- with the CLAS detector.

In Fig. 10, we show the variation of the main kinematical parameters of scattered electrons and recoil protons (p_f).

For more detailed information, as well as for including the effects of Fermi motion, a Monte-Carlo calculation was carried out. Since the $Q^2 = 4(\text{GeV}/c)^2$ point is most important, we consider the results obtained for this case, only.

In Fig. 11, the angular distributions (with respect to the direction of the virtual photon) of the recoil protons before (p_f) and after (p'_f) secondary elastic scattering under different conditions are displayed for $Q^2 = 4 \pm 1(\text{GeV}/c)^2$. For both processes - electron quasi-elastic scattering ($0.76 \leq W^2 \leq 0.92\text{GeV}^2$) and secondary elastic scattering of the recoil proton - the same Fermi momentum distribution (with $p_F = 0.16\text{GeV}/c$) for the ${}^4\text{He}$ nucleus was used. One can see an angular spread (mainly due to the Fermi motion) of $\approx \pm 3^\circ$ which is almost the same for both non-interacting and elastically scattered protons. In Fig. 11d, the distribution of the protons from inelastic electron-nucleus interaction is displayed. One can see that contribution from this process in the quasi-elastic region does not exceed 1%.

In Fig. 12, the same angular distributions are given for the elastically scattered (p'_f) and secondary recoil (p_r) protons, with and without cuts in the momentum of the secondary recoil proton. Setting an upper limit of $p_r \leq 0.55\text{GeV}/c$ eliminates the contribution from the inelastic proton-nucleon interaction ($E_f + m - E'_f \leq m_\pi$). The lower limit $p_r \geq 0.3\text{GeV}/c$ is necessary to eliminate evaporation protons. These cuts do not change the shape of the angular distribution of the scattered protons. There is a small suppression of secondary recoil protons at large angles. Note that the contribution from nucleon pair correlations (which is the main background process) is expected to be small due to the small Fermi momenta considered ($p_i \leq 0.16\text{GeV}/c$). For the further suppression of this contribution the angular region $\theta_{r,q} \leq 90^\circ$ can be used. Thus, the kinematic region for the secondary recoil protons is defined: $10^\circ \leq \theta_{r,q} \leq 90^\circ$ and $0.3 \leq p_r \leq 0.55\text{GeV}/c$.

To obtain the momentum region of the elastically scattered protons, the dependences of the Monte-Carlo generated events on the quantity $p_f - q$ are displayed in Fig. 13.

In Fig. 14, the same momentum spectra are given with the cuts to the momentum p_r .

mentioned above. This shows that the momentum interval for scattered protons is about 150 MeV/c wide (namely, the interval $(q - 0.1) \leq p_f(p'_f) \leq (q + 0.05)GeV/c$).

The intervals for the kinematic parameters of the reactions (4) and (5) are now completely defined:

$$\begin{aligned}
15^\circ \leq \theta_{e'} \leq 43^\circ, \quad 1.5 \leq E_{e'} \leq 4GeV \\
\theta_q - 5^\circ \leq \theta_{fq} \leq \theta_q + 5^\circ, \quad (q - 0.1) \leq p_f \leq (q + 0.05)GeV/c \\
10^\circ \leq \theta_{rq} \leq 90^\circ, \quad 0.3 \leq p_r \leq 0.55GeV/c
\end{aligned} \tag{10}$$

In Fig. 15, the kinematic conditions discussed above are illustrated. In the "forward" cone of the proton arm both the non-scattered or the elastically (once) scattered protons have to be detected, whereas the secondary recoil protons will be recorded in the "backward" cone.

4. The Counting Rate

For counting rate estimates, experimental data for the quasi-elastic $^{12}C(e, e'p)$ reaction obtained at Yerevan [17] can be used. In Fig. 16, the $E_{e'}$ spectra at $E_e = 2.0GeV$ and $Q^2 = 0.25(GeV/c)^2$ are presented. The solid curve shows theoretical calculations [18] in the Light Cone approximation. According to these data, the cross section at the quasi-elastic peak is $\approx 6 \cdot 10^{-30} cm^2/sr \cdot GeV/nucleus = 1 \cdot 10^{-30} cm^2/sr \cdot GeV/proton$.

Since in the proposed experiment the counting rate rate limitation occurs at $Q^2 = 4(GeV/c)^2$, the counting rate must be determined for this Q^2 point. To obtain the corresponding cross section we use the dipole form-factor to describe the Q^2 dependence:

$$\frac{d^2\sigma}{d\Omega_{e'}dE_{e'}} \sim \frac{E_{e'}^2}{Q^4} \cdot \frac{\cos^2\theta_{e'}/2}{(1 + Q^2/0.71)^4} \tag{11}$$

According to Eq.(11), $d^2\sigma(Q^2 = 4) = 0.7 \cdot 10^{-5} \cdot d^2\sigma(Q^2 = 0.25)$, since $E_{e'}(Q^2 = 0.25) = 1.84GeV$, $\theta_{e'}(Q^2 = 0.25) = 15^\circ$; $E_{e'}(Q^2 = 4) = 1.88GeV$, $\theta_{e'}(Q^2 = 4) = 43^\circ$. Therefore,

$$\frac{d^2\sigma}{d\Omega_{e'}dE_{e'}}(Q^2 = 4) \approx 0.7 \cdot 10^{-35}/sr \cdot GeV/proton$$

For the bin sizes $\Delta E_{e'} = 0.2GeV$, $\Delta\theta_{e'} = 2^\circ$, and $\Delta\phi_{e'} = 2\pi$ which correspond to $\Delta\Omega_{e'} \approx 0.15sr$, $\Delta Q^2 \approx 0.6(GeV/c)^2$ (at $Q^2 = 4(GeV/c)^2$ and $\theta_{e'} = 43^\circ$), and at a luminosity of $L = 10^{34}/cm^2sec$ [19],

$$N_{e,e'p_f} \approx 7.2/hour \quad (12)$$

The corresponding counting rate for three-particle coincidence events is

$$N_{e,e'p_f p_r} \geq 0.1/hour$$

The reduction (by a factor ~ 30) of the rate $N_{e,e'p_f p_r}$ with respect to $N_{e,e'p_f}$ is due to:

$N_{tot} = \frac{1}{1.5} \cdot N_R$; $N_{tot}^{el} = \frac{1}{3} \cdot N_{tot}$; $N_{pp}^{el} = \frac{1}{3} \cdot N_{tot}^{el}$; $N_{pp}^{el}(10^\circ \leq \theta_{rq} \leq 90^\circ, 0.3 \leq p_r \leq 0.55 GeV/c) \approx \frac{1}{1.5} \cdot N_{pp}^{el}$ (see Fig. 11 and 12), and due to the 50% acceptance of the CLAS at $Q^2 = 4 GeV$ (see below).

4. Acceptance

The topology of double-scattering events is shown in the single event display in Fig. 17. The proton from the initial electron scattering is emitted with high energy into the forward cone. The second proton is of lower energy but is detected with high efficiency since it scatters through larger angles. The CLAS geometry is well suited for the detection of this event topology, as shown in Fig. 18. The uniform acceptance for double-scattering events is shown as a function of Q^2 and momentum transfer t . At the highest Q^2 , where the rates are low, the efficiency reaches 50%.

5. Beam Time Request

To accumulate 50 events at $Q^2 = 4(GeV/c)^2$ ($\pm 15\%$ statistical error bars) a run time of 300 hours of beam time is required. A 60 hour run under similar conditions has already been approved previously (Multi-hadron Working Group proposals PR-89-015, -017, -027, -031, -032 and -036), so this request is for an additional 240 hours. In Fig. 19, we show the expected experimental results due to Color Transparency in a 4He nucleus which can be obtained during this running time.

References

1. L.L. Frankfurt, G.A. Miller, and M.I. Strikman, *Comments on Particle and Nuclear Physics*, v.21, p.1(1993).
2. L.L. Frankfurt, G.A. Miller, and M.I. Strikman, *Nucl. Phys.A*, in press.
3. S.J. Brodsky, in *Proceedings of the Thirteenth International Symposium on Multiparticle Dynamics*, edited by E.W. Kittel, W. Metzger, and A. Stergiou (World Scientific, Singapore, 1982), p.964.
4. A. Mueller, in *Proceedings of the 17 Rencontre de Moriond* edited by J. Tranh Thanh Van (Editions Frontieres, Gif-sur-Yvette, 1982), p.13.
5. G.R. Farrar, L.L. Frankfurt, M.I. Strikman and H. Liu, *Phys. Rev. Lett.*, **61**, 686(1988).
6. B.K. Jennings and G.A. Miller, *Phys. Lett.*, **B236**, 209(1990); B.K. Jennings and G.A. Miller, *Phys. Rev.*, **D 44**, 692(1991); *Phys. Rev. Lett.*, **70**, 3619(1992); *Phys. Lett.*, **B274**, 442(1992).
7. L.L. Frankfurt, M.I. Strikman and M. Zhalov, *Nucl. Phys.*, **A515**, 599(1990).
8. J.P. Ralston and B. Pire, *Phys. Rev. Lett.*, **61**, 1823(1988). B. Pire and J.P. Ralston, *Phys. Lett.*, **117B**, 233(1982)
9. O. Benhar et al. *Phys. Rev. Lett.*, v.69, 881(1992).
10. A.S. Carroll et al. *Phys. Rev. Lett.*, **61**, 1698(1988).
11. SLAC experiment NE-18, R. Milner, spokesman.
12. A.S. Carroll et al., BNL experiment 850.
13. L.L. Frankfurt and M.I. Strikman, in *Particle and Nuclear Physics*, v.27, p.135(1991).
14. L.L. Frankfurt and M.I. Strikman, *Nucl. Phys.*, **B250**, p.143(1985)
15. K.Sh. Egiyan, L.L. Frankfurt, W.R. Greenberg, G.A. Miller, M.M. Sargsyan, and M.I. Strikman, CEBAF Preprint, PR-93-002.
16. L.L. Frankfurt, W.R. Greenberg, G.A. Miller, and M.I. Strikman, *Phys. Rev.*, **C46**, 2547(1992).
17. K.V. Alanakyan, M.J. Amaryan, G.A. Asryan et al., Preprint YerPI, YERPHI-1303(89)-90.
18. M.M. Sargsyan, Preprint YerPI, YERPH-1331(26)-91
19. CEBAF Conceptual Design Report, April 13, 1990 (Revised).

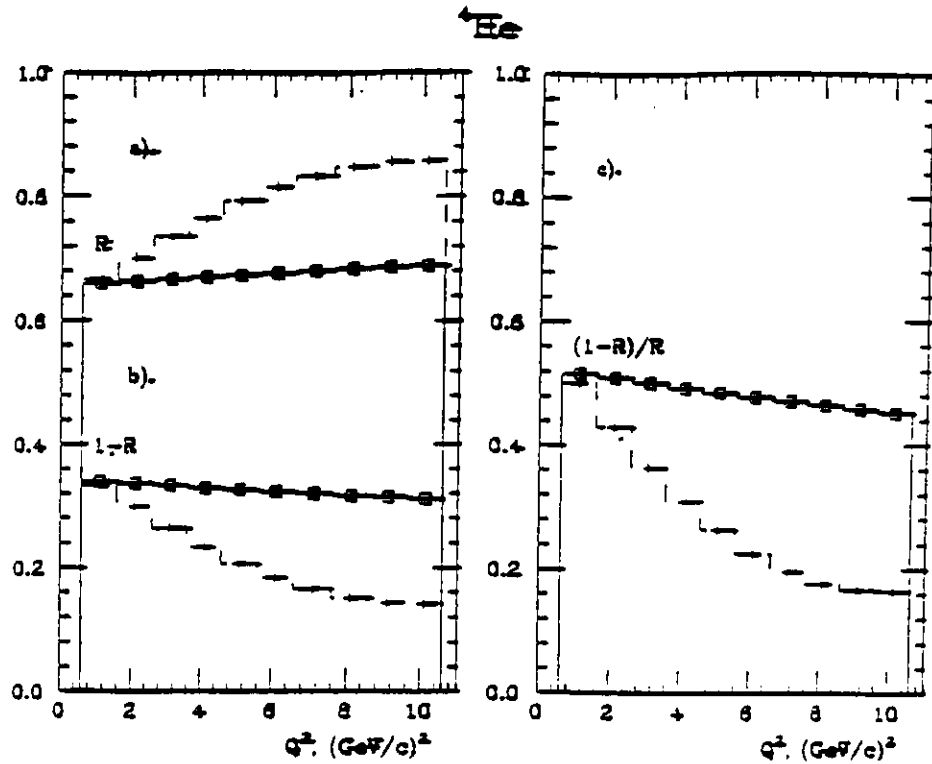


Fig.2 Calculated Q^2 dependences of Color Transparency effect for ${}^4\text{He}$ nucleus. Dashed and solid histograms represent the results with and without CT effect.

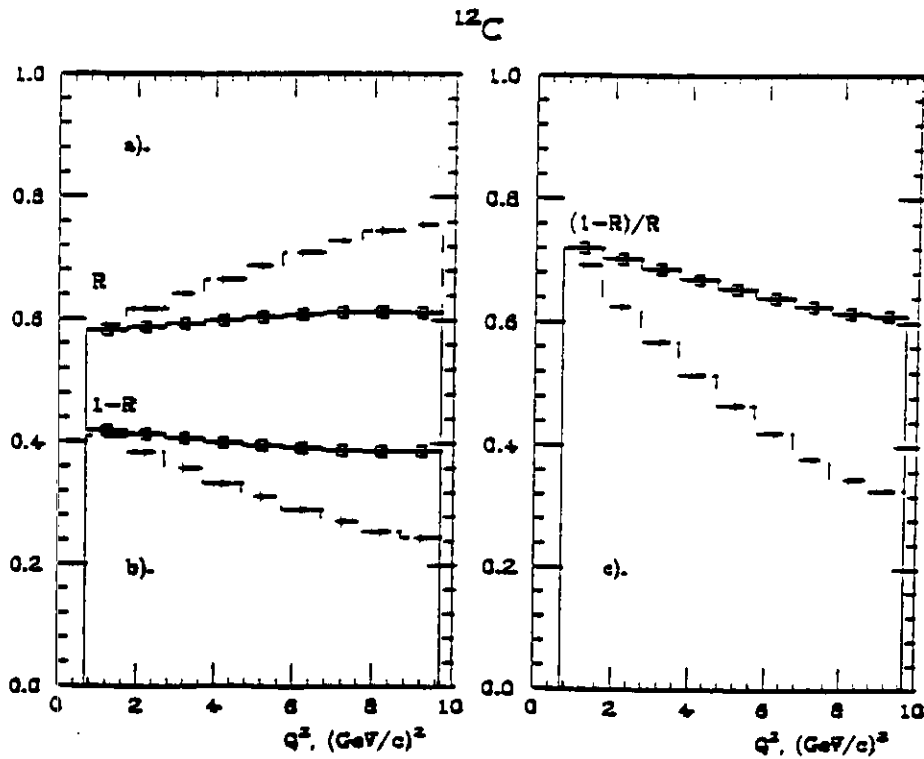


Fig.3 The same as Fig.2, for ${}^{12}\text{C}$ nucleus.

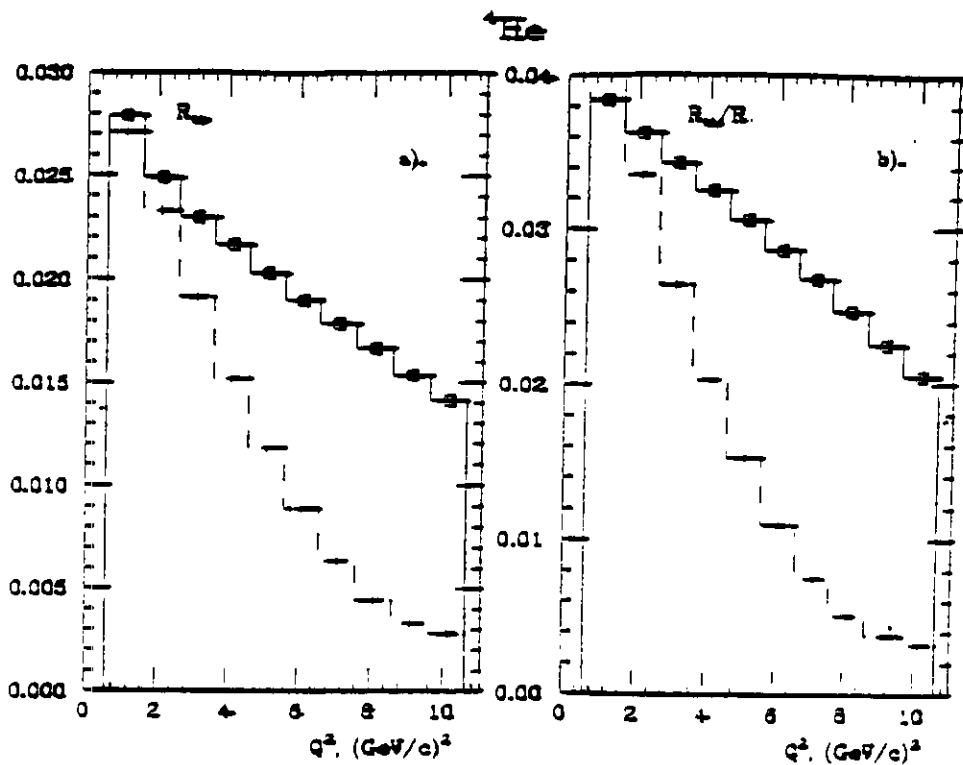


Fig.4 The same as Fig.2 for elastic channel of recoil proton scattering off individual protons in A-1 system.

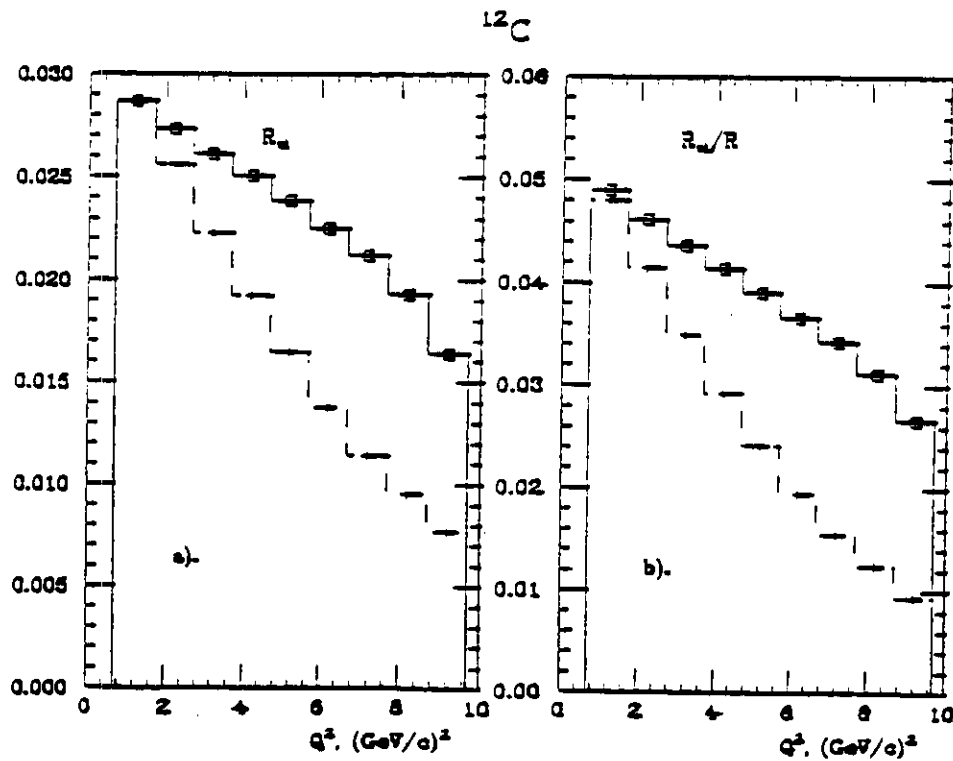


Fig.5 The same as Fig.4 for ${}^{12}\text{C}$ nucleus.

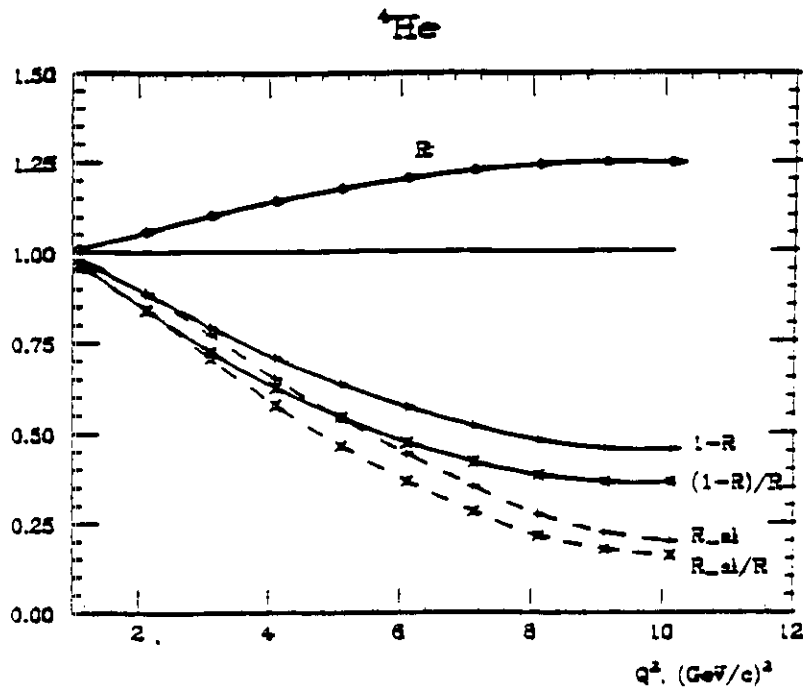


Fig.6 The Q^2 dependences of a quantities R , $1 - R$, $\frac{1-R}{R}$, R_{el} and $\frac{R_{el}}{R}$, normalized to the corresponding Glauber calculations, for ${}^4\text{He}$ nucleus.

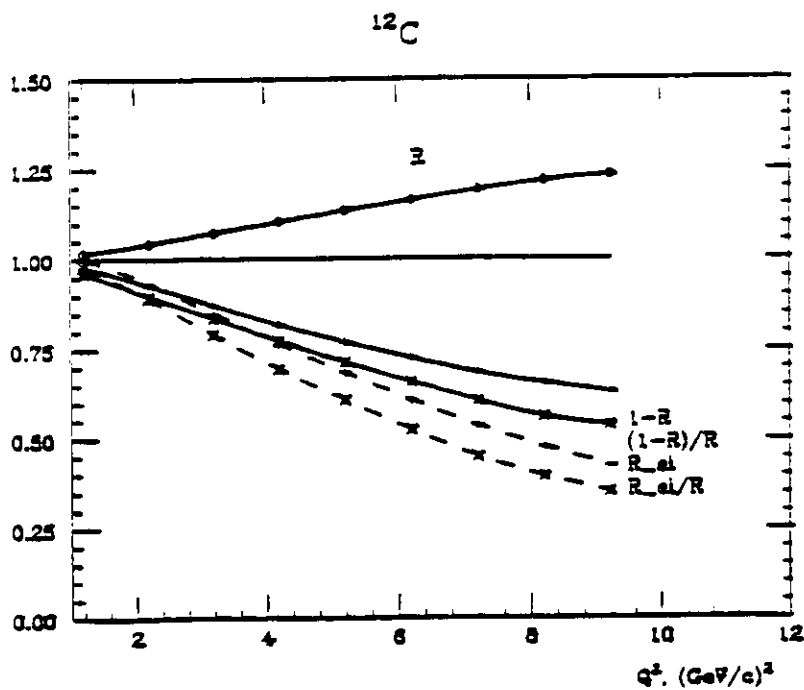


Fig.7 The same as Fig.6, for ${}^{12}\text{C}$ nucleus.

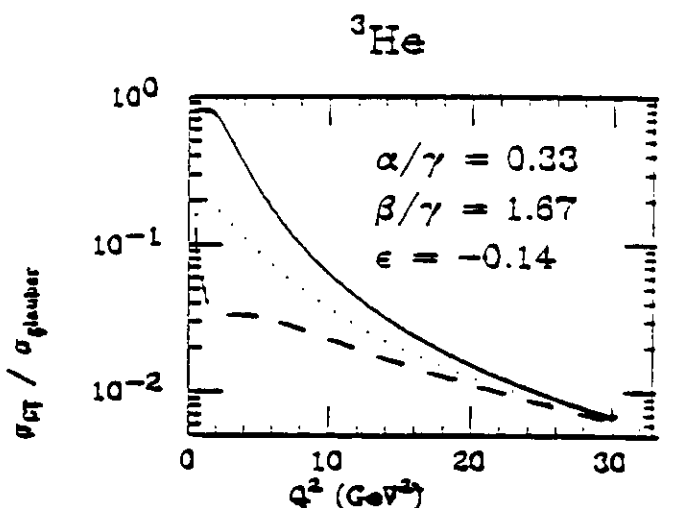
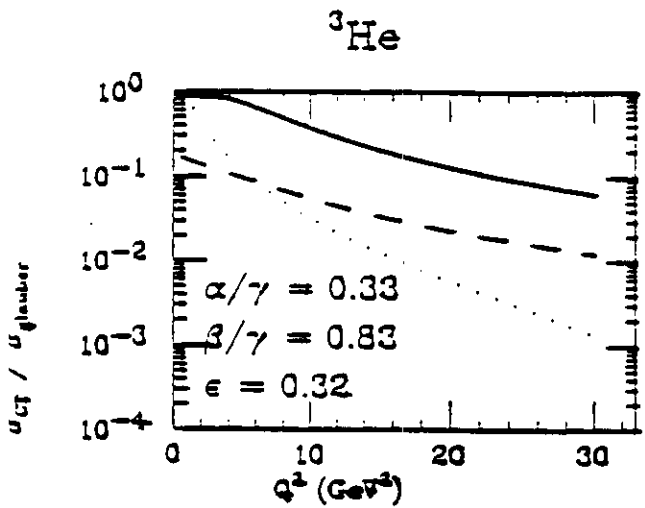
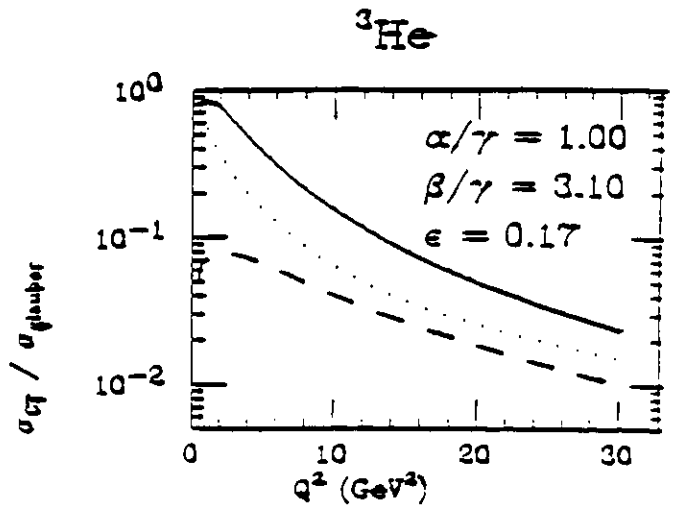
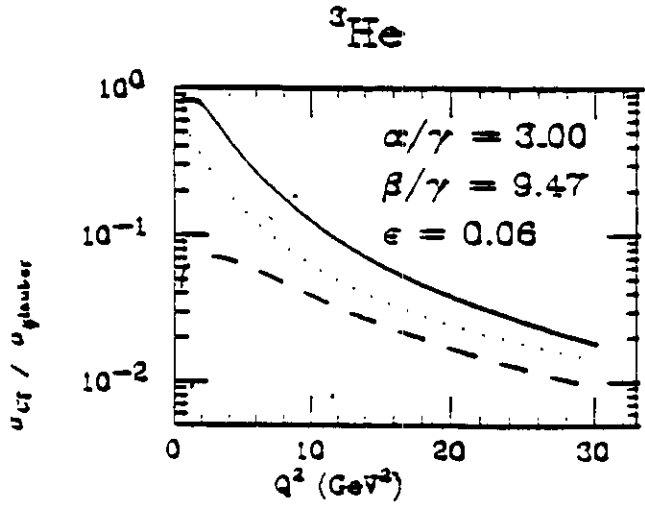


Fig. 8 Ratio of cross sections for the reaction of Eq. (10) for color transparency (CT) or conventional calculation ("Glauber"). Solid: quasielastic proton production. Dashed: quasielastic $N^*(1.4 \text{ GeV})$ production. Dotted: quasielastic $N^{**}(1.8 \text{ GeV})$ production. The parameters α, β, γ and ϵ define the baryon-nucleon soft interaction, see Ref.15.

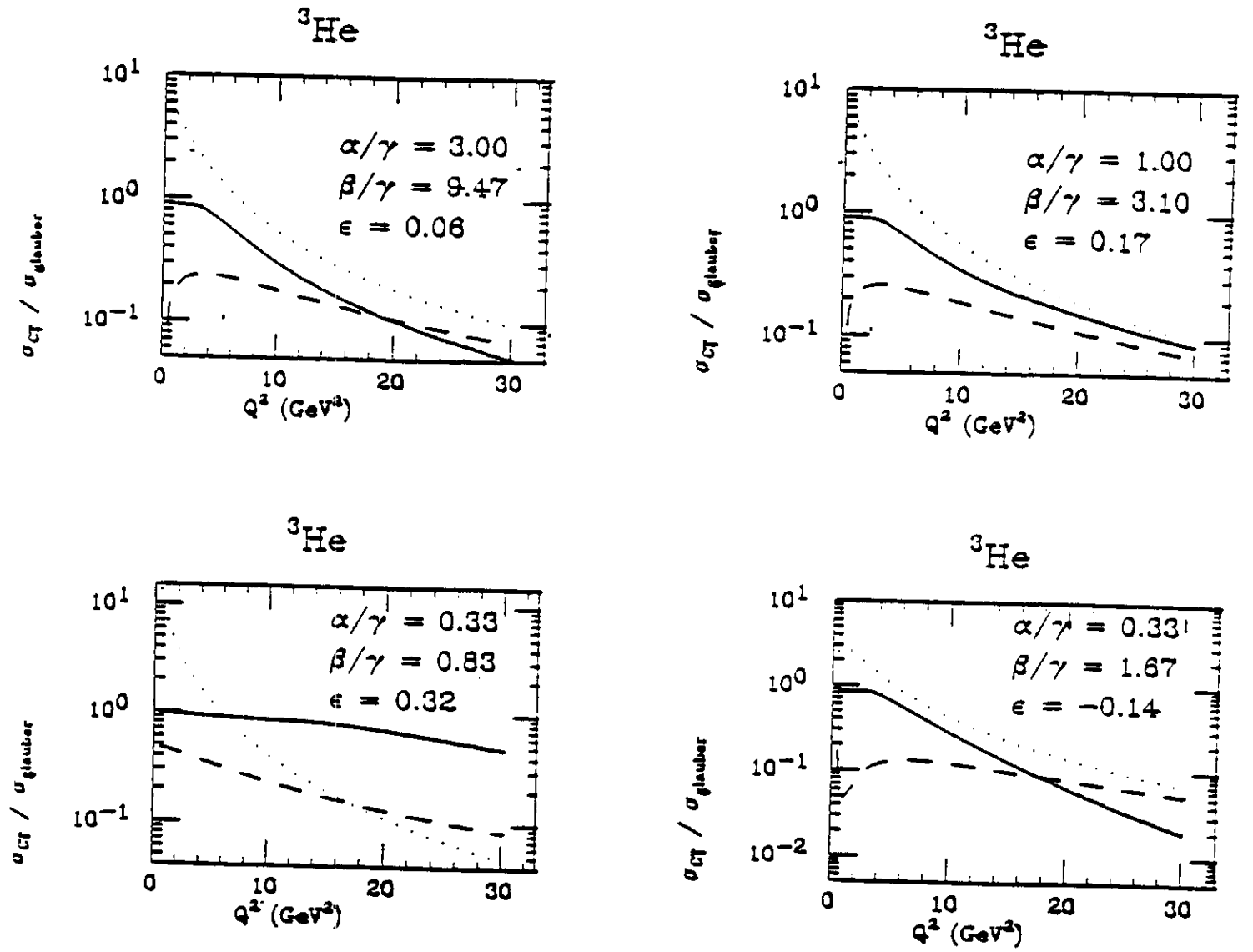


Fig. 9 Same as Fig.8, but the masses are $(N^*, N^{**}) = (1.7, 3 \text{ GeV})$

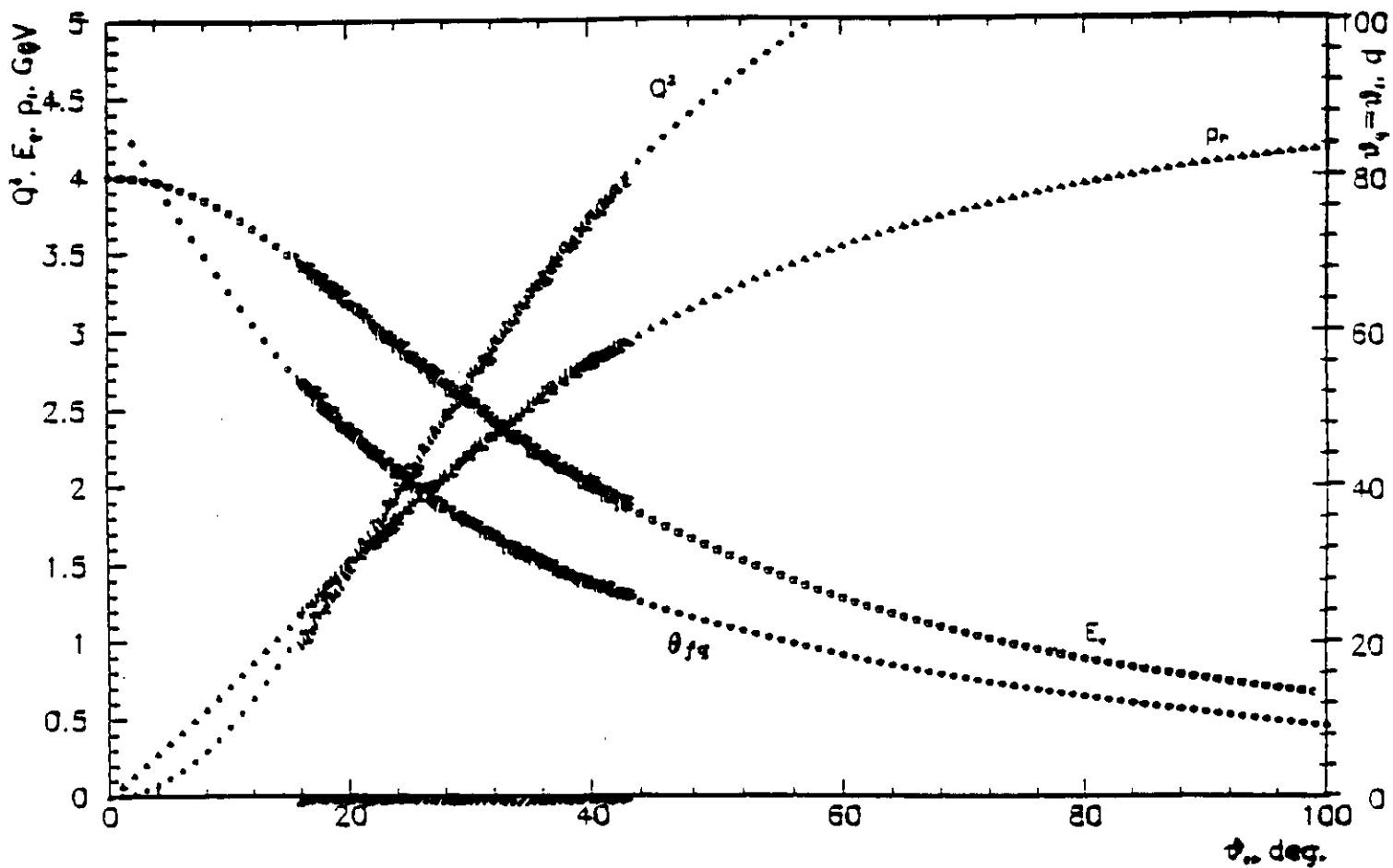


Fig. 10 Dependences of the Q^2, p_e, p_{fq} and $\theta_q = \theta_f$ on θ_e at $E_e = 4 \text{ GeV}$. The curves are dashed in the regions, corresponding to the $Q^2 = 1 \div 4 (\text{GeV}/c)^2$ interval.

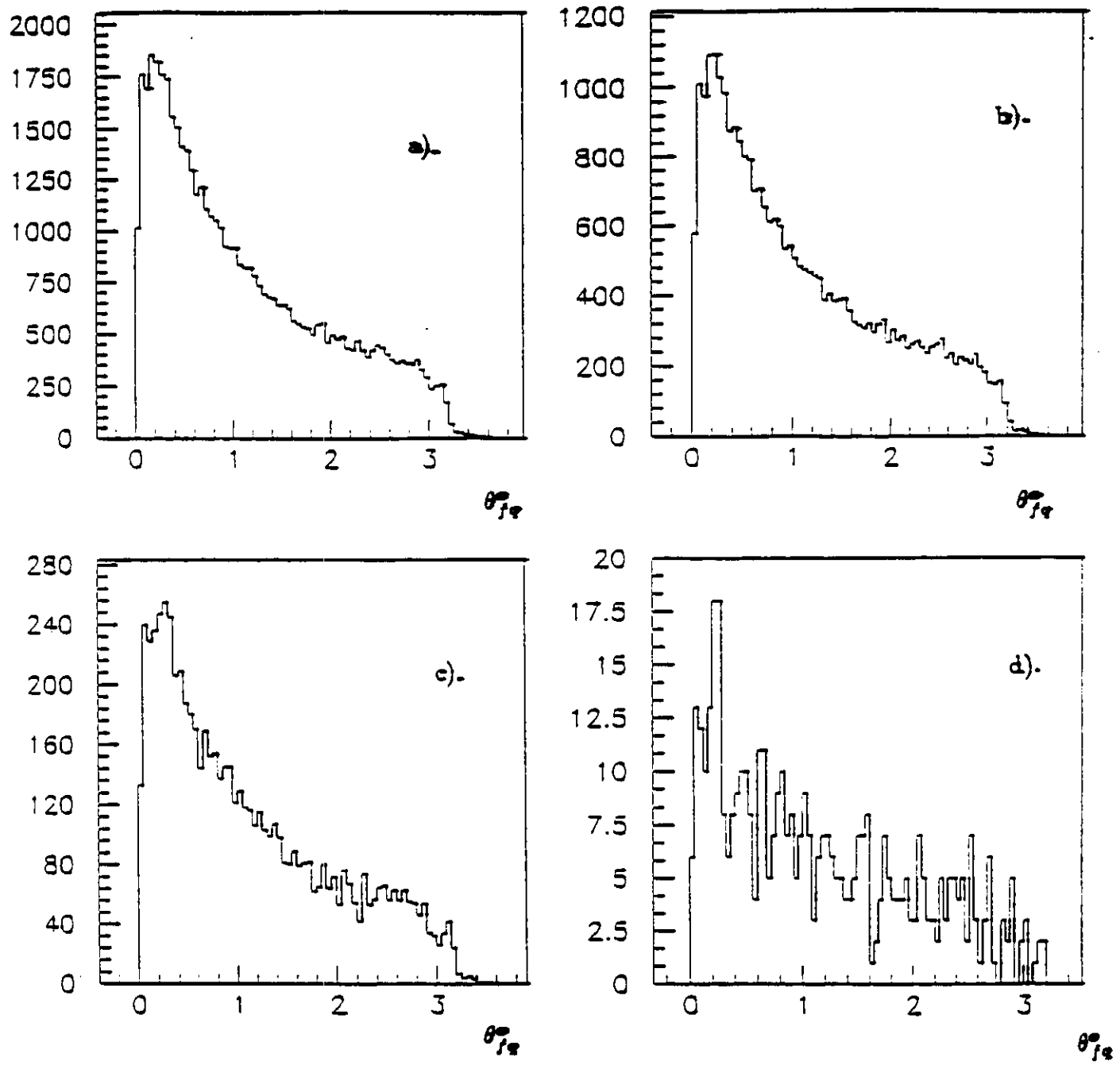


Fig.11 Angular distributions of: all elastic recoil protons (a), without (b), with (c) secondary elastic scattering, and protons from the inelastic electron interaction on the 4He nucleus (d). Fermi momentum distribution with $p_F = 0.16 GeV/c$ was used.

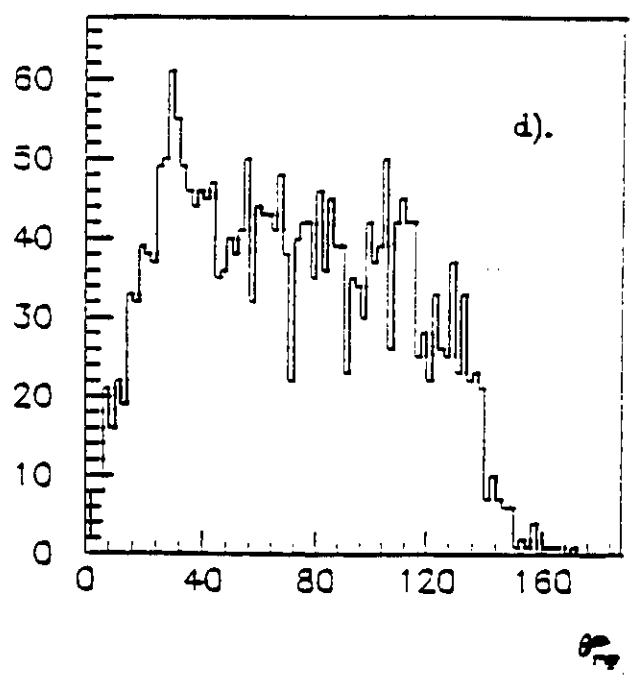
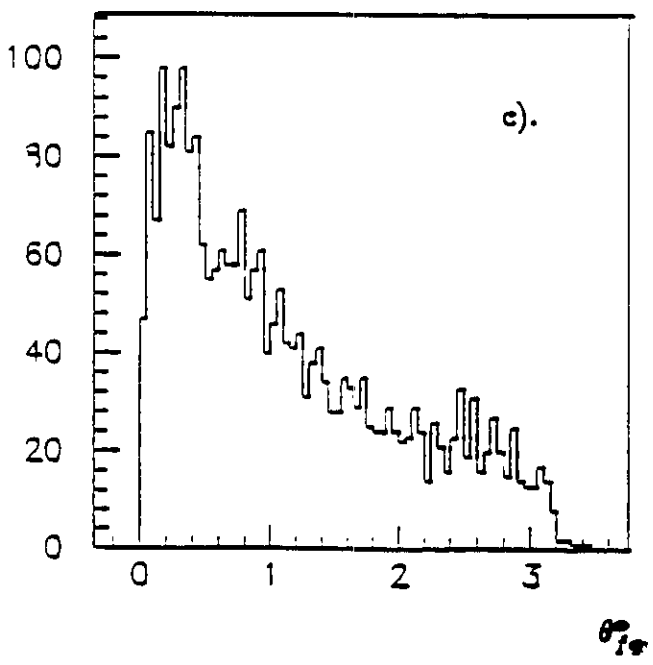
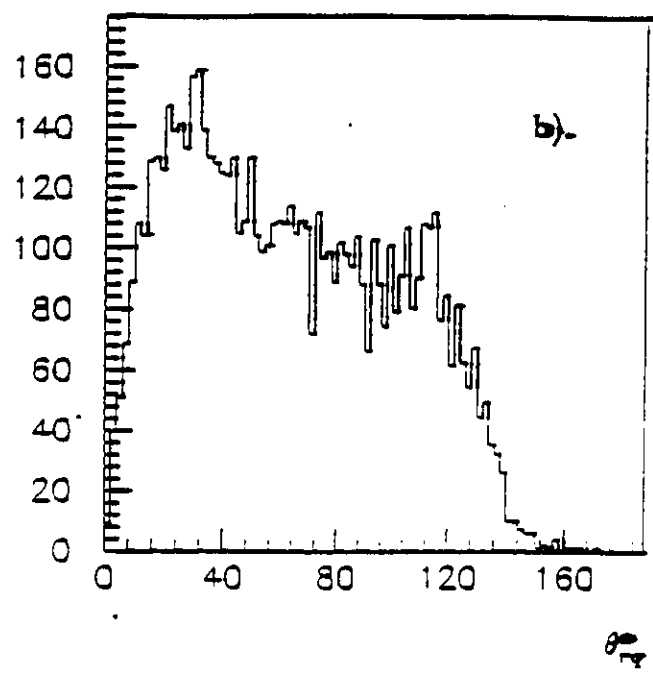
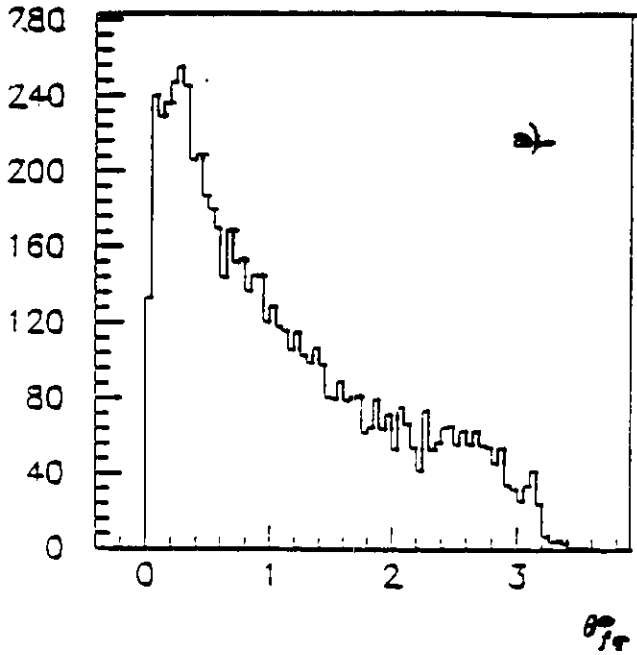


Fig.12 Angular distributions of the elastically scattered (a, c) and secondary recoil protons (b, d) without (a, b) and with (c, d) momentum $0.3 \leq p_r \leq 0.55 \text{ GeV}/c$ limitations.

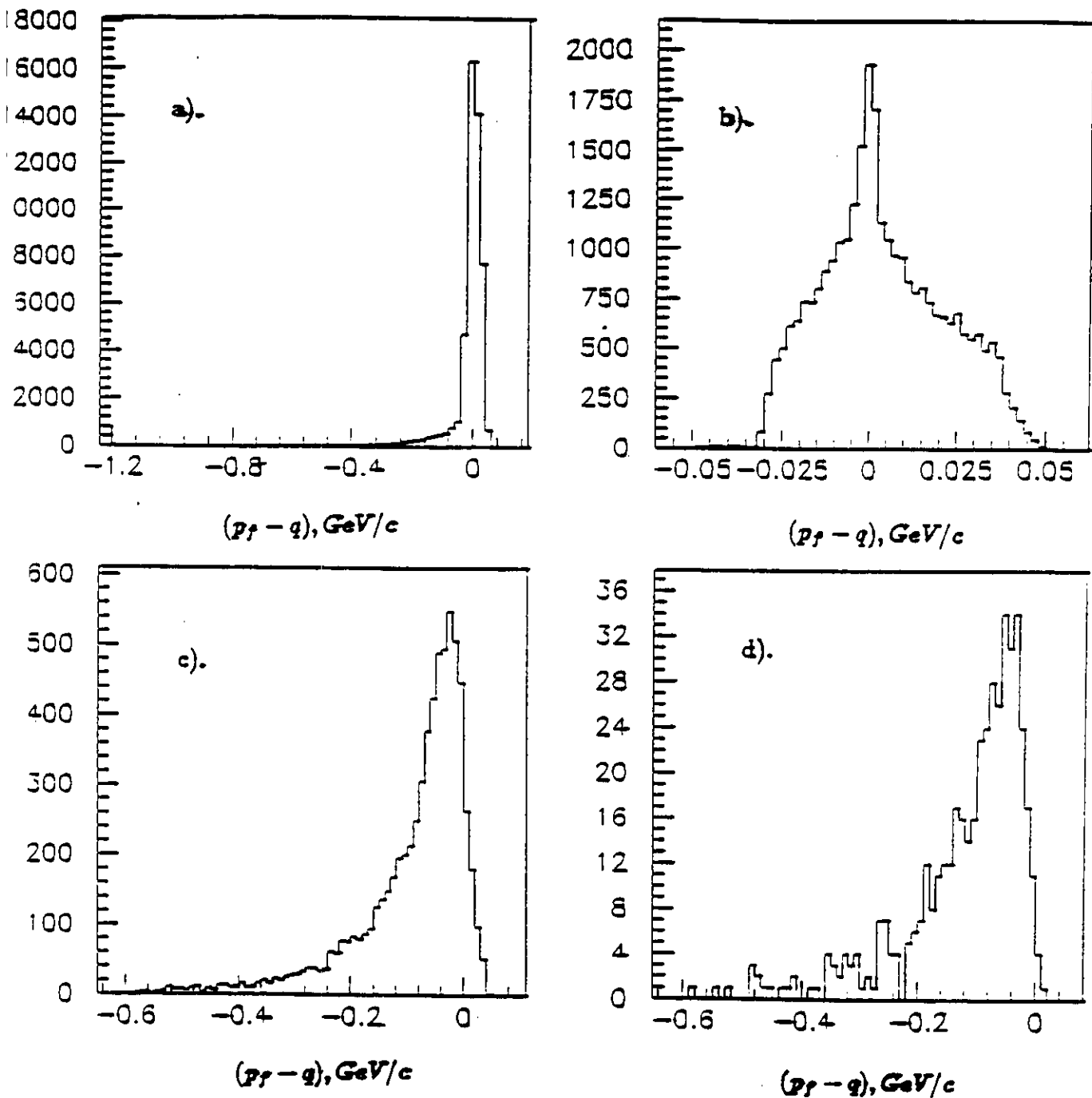
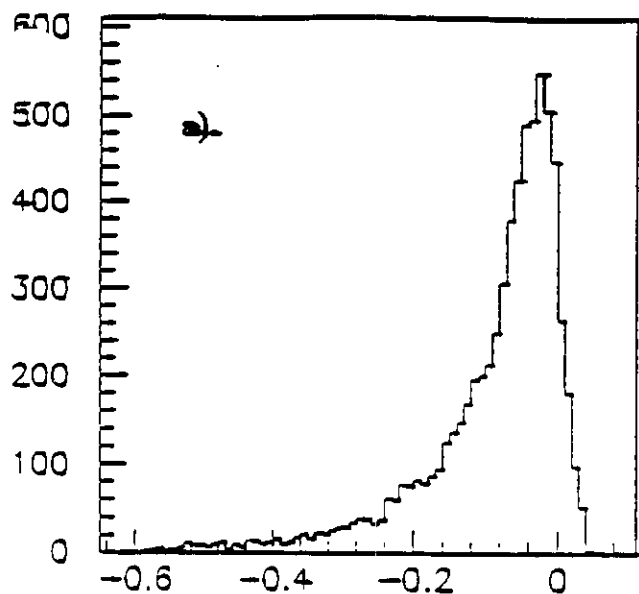
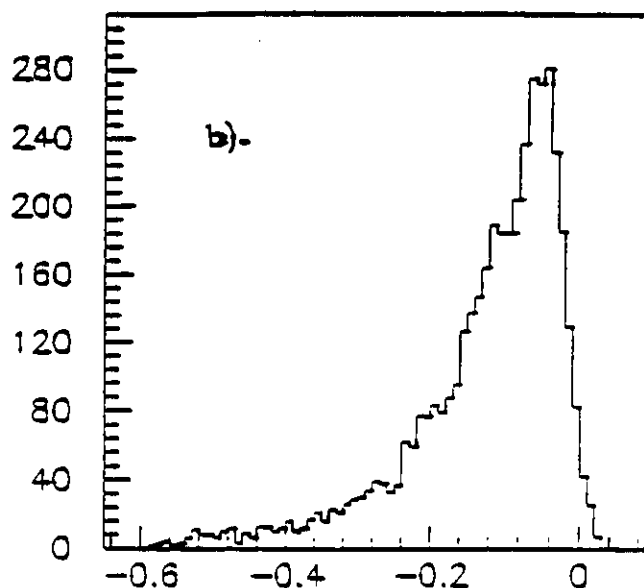


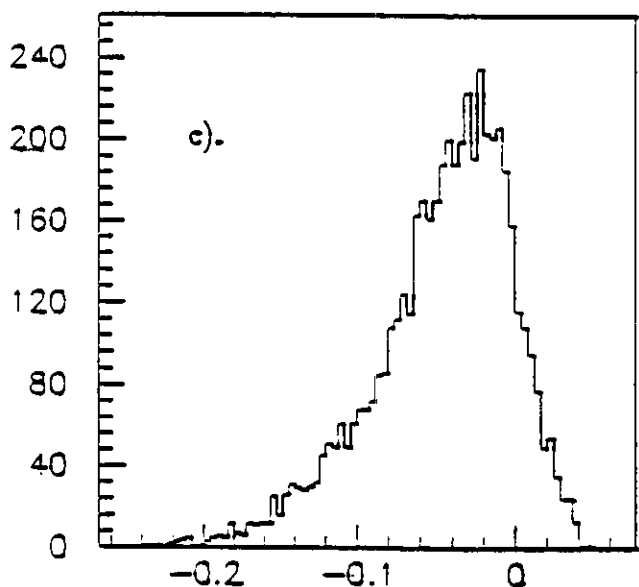
Fig.13 Monte-Carlo event dependences from the value $(p_f - q)$ for all recoil (a), noninteracted (b), elastically scattered (c) protons from the quasielastic electron scattering and for the protons from the inelastic electron interaction (d). Fermi momentum distribution with $p_F = 0.16 \text{GeV}/c$ was used.



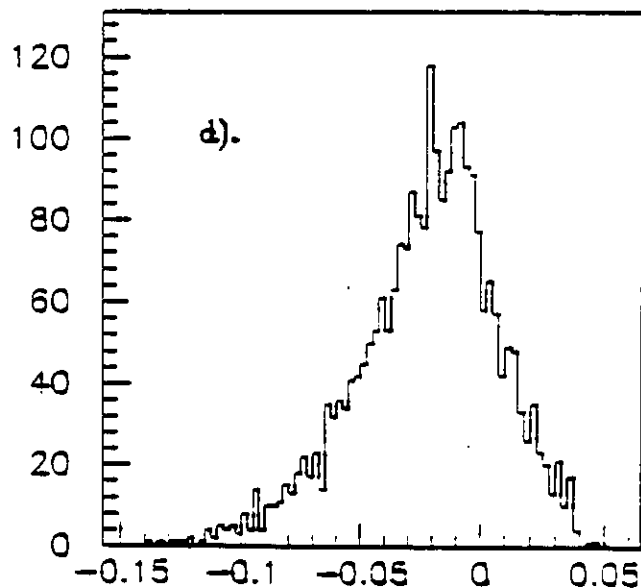
(a) $(p_f - q), \text{GeV}/c$



(b) $(p_f - q), \text{GeV}/c$



(c) $(p_f - q), \text{GeV}/c$



(d) $(p_f - q), \text{GeV}/c$

Fig.14 The same as in Fig. 13, for all elastically scattered protons (a), after $p_r \geq 0.3 \text{GeV}/c$ (b), $p_r \leq q - 0.15 \text{GeV}/c$ (c) and $0.3 \leq p_r \leq q - 0.15 \text{GeV}/c$ (d) limitations.

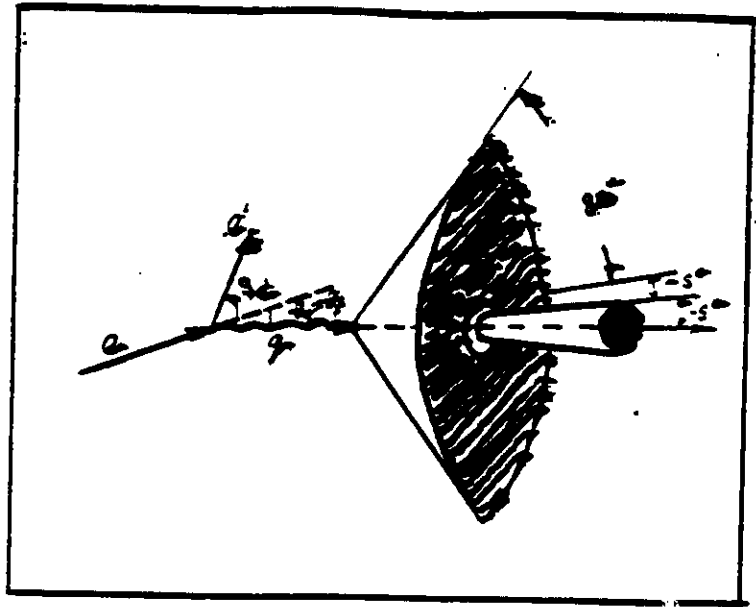


Fig.15 Kinematics of the reaction (5). In the "forward" cone the nonscattered and/or (once) elastically scattered protons have to be detected, as in the "backward" cone the secondary recoil protons will be registered.

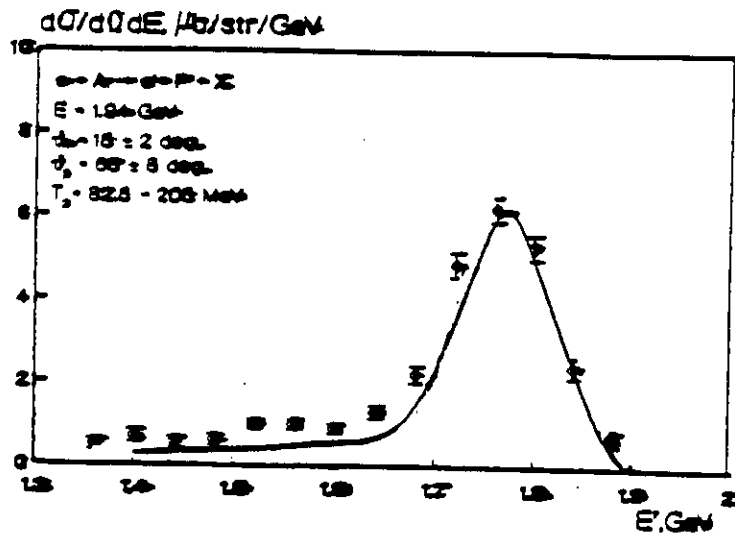


Fig.16 Experimental data [17] of the quasielastic ($e, e'p_f$) measurements at the $E_e = 2.0 \text{ GeV}$, $Q^2 = 0.25 (\text{GeV}/c)^2$. Solid line represent the theoretical calculations [18] in the Light Cone approximation. measured simultaneously.

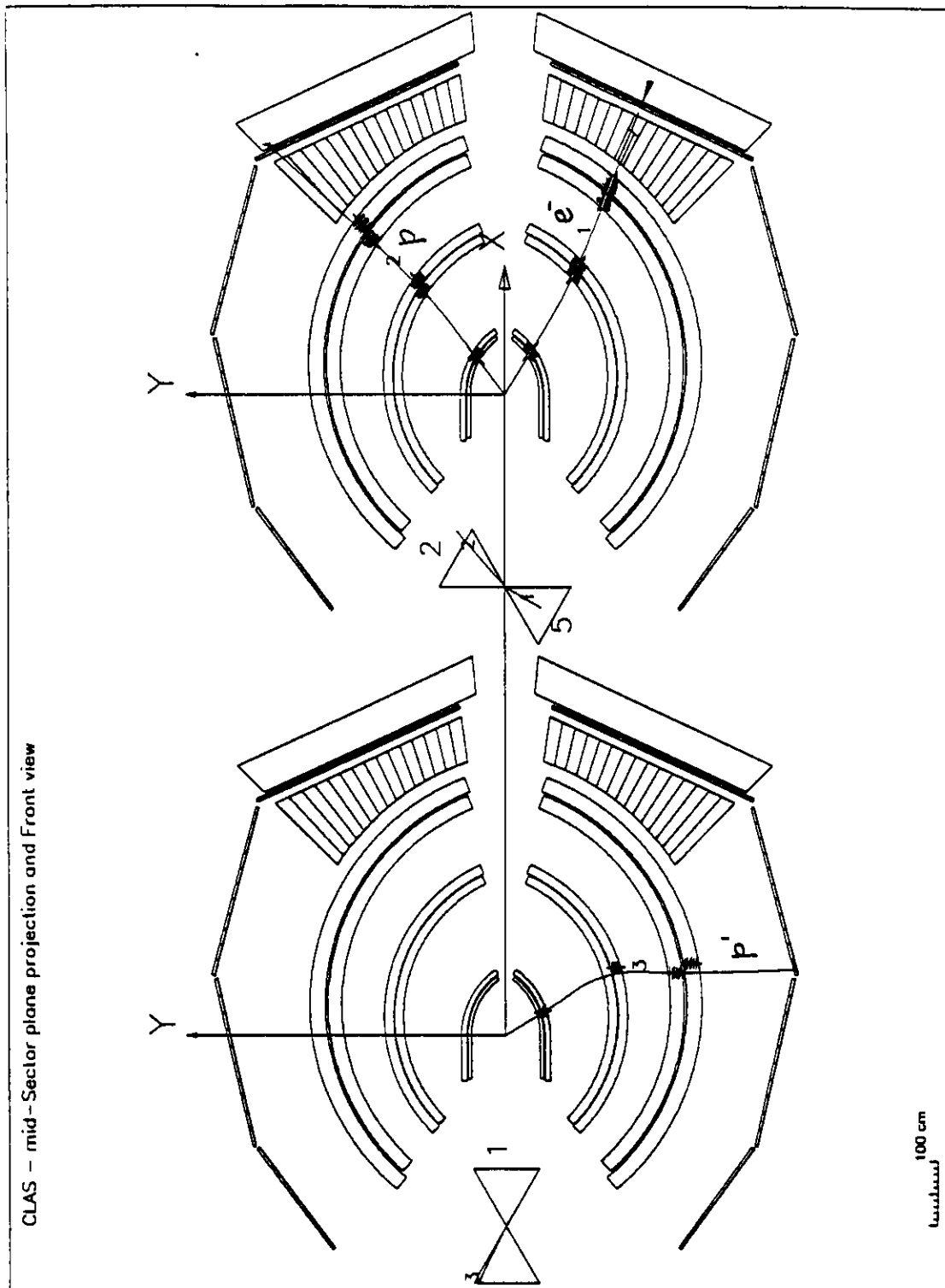


Fig. 17 Single event display showing the electron, and two protons in two opposite sectors of the CLAS detector.

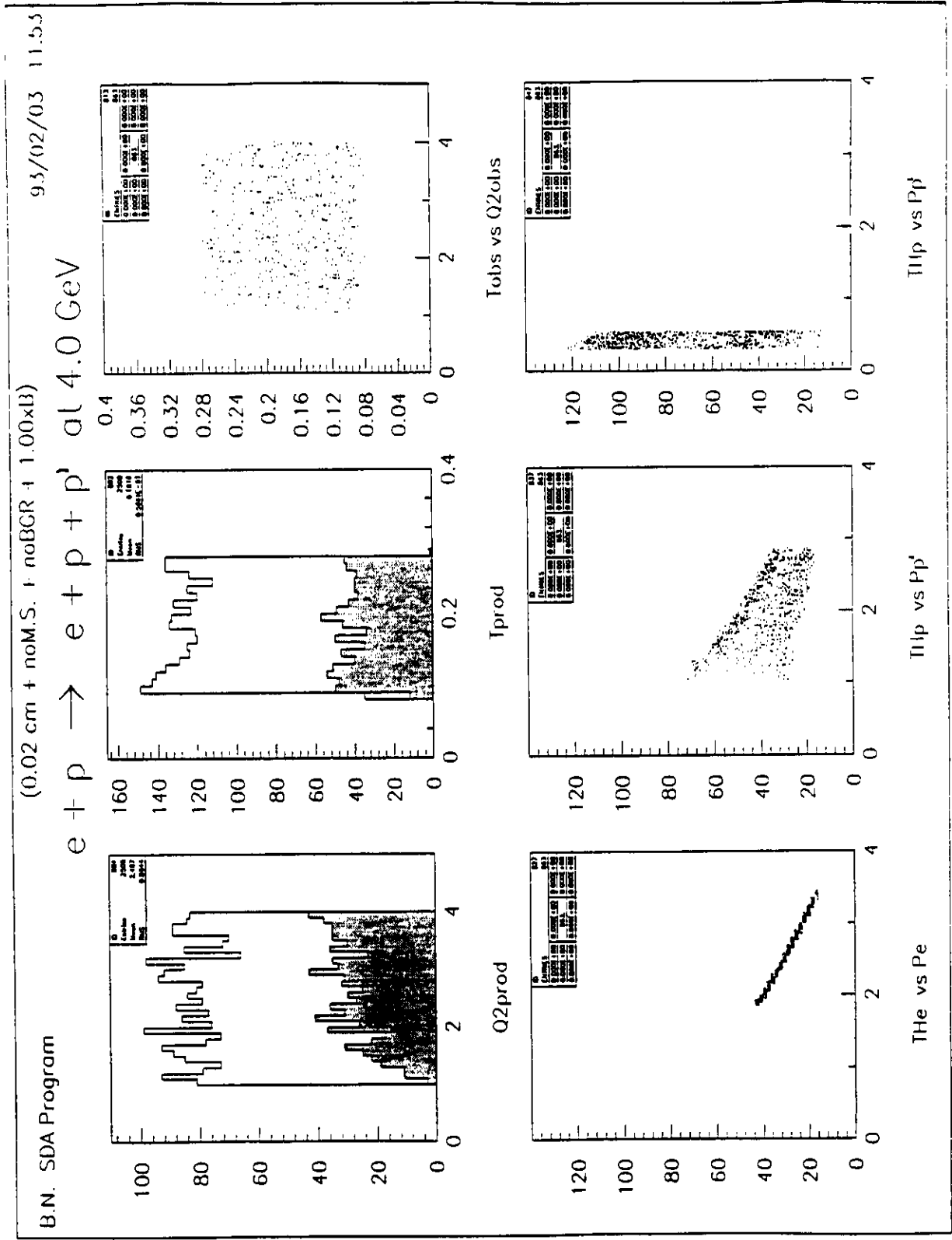


Fig. 18 Acceptance of double-scattering events in the CLAS detector as a function of Q^2 and momentum transfer t . The range of angles and momenta of the electron and two protons is also shown.

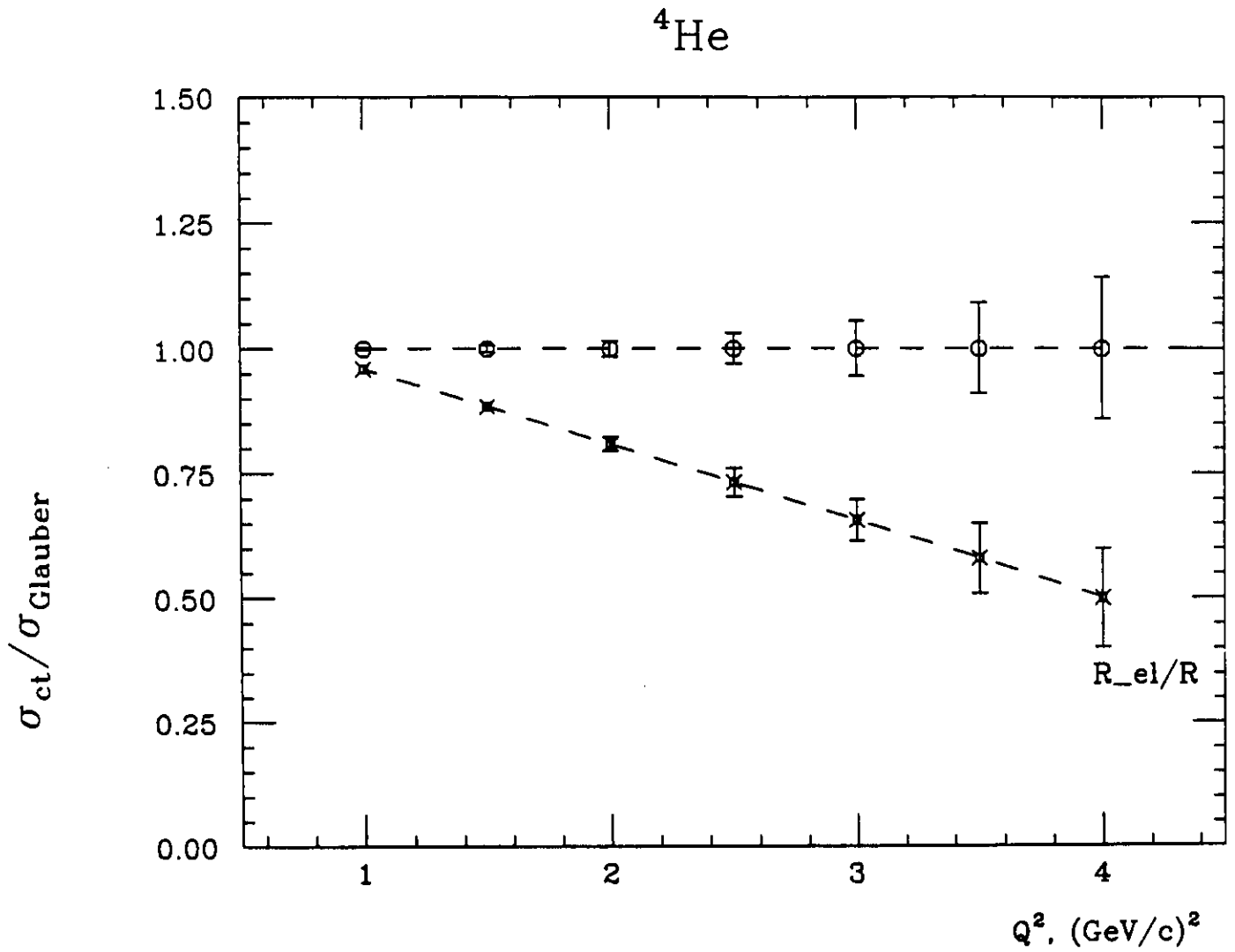


Fig. 19 Expected results of the Color Transparency effect in ${}^4\text{He}$ using 300 hours of beam-time. Open circles - without, cross symbols - with Color Transparency effect.